Models for Estimation of Pure *n*-Alkanes' Thermodynamic Properties as a Function of Carbon Chain Length

Anne-Julie Briard, Mohammed Bouroukba, Dominique Petitjean, and Michel Dirand*

Laboratoire de Thermodynamique des Milieux Polyphasés EA n*o*. 3099, Ecole Nationale Supérieure des Industries Chimiques, Institut National Polytechnique de Lorraine, 1, rue Grandville, BP 451, F-54001 Nancy Cedex, France

Simple predictive relationships for the estimation of pure normal alkanes' thermodynamic properties, like transition temperatures, phase change enthalpies, and heat capacities in the solid or liquid state, are established as a function of carbon atom number n_c, by combining our own calorimetric experimental results and a general review of literature data. This study underlines that total and melting enthalpies vary linearly with n_c carbon atom number, whatever the parity of n_c, while order−disorder transition enthalpies show a quadratic variation and an alternating effect between odd- and even-numbered *n*-alkanes. Heat capacity variations versus temperature and the carbon chain length were represented by a model of group contributions for the liquid phase and by an expression derived from Einstein's model for the solid state.

Introduction

The crystallization of heavy hydrocarbons in the fluids of paraffinic crude and middle distillate fuels has been shown to be at the origin of real problems for refiners and diesel-fuel consumers in very cold regions. The accumulation of these solid deposits, which clog up filters and obstruct pipelines during production or transport, could lead to the damage of industrial equipment and diesel motors. To solve these problems, it is essential to develop a thermodynamic model which is able to predict the conditions of paraffin deposit crystallization for a given fluid composition and for a given temperature. Determining the solid deposit curves requires the knowledge of all thermodynamic data of pure compounds occurring in the solid/liquid equilibrium. To facilitate collecting these thermodynamic properties, to remedy to the lack of literature data, and to simplify the thermodynamic model use, predictive relations between *n*-alkanes phase change properties and carbon chain length would be very useful tools. So, the aim of this paper is to establish these relations by combining a great number of literature and experimental results, obtained in a large chain length range ($4 \leq n_c \leq 390$).

n-Alkanes' Structural Behavior

Despite a rather simple molecular structure, *n*-alkanes (hereafter denoted by C_n with *n* the carbon atom number of the chain) reveal a very significant polymorphism and many allotropic transformations, the structure of the phase being governed by three parameters: the temperature, the parity, and the carbon atom number of the chain.

C_n's Crystalline Ordered Structures of Low Temperatures. The crystallographic structures of low temperature ordered phases of C_n's have been specified by Craig et al.[1] and by Chevallier et al.[2] Craig et al.[1] have determined the unit-cell crystallographic parameters and space groups of the homologous series C_{13}−C_{60} by high-resolution synchrotron X-ray powder diffraction, and Chevallier et al.,[2] the correlations between the crystalline long *c*-parameter of the unit-cell, directed along the C_n carbon chains, and the n_c carbon atom number. Tables 1 and 2 summarize all crystalline structures observed before any solid−solid transition respectively for odd- and even-numbered C_n's, as a function of chain length.

Table 1. Odd-Numbered C_{2p+1}'s Structures as a Function of Chain Length n_c

n_c range	structure	space group	coordination number *Z*
$5 \leq n_c \leq 7$	triclinic	$P\bar{1}$	2
$9 \leq n_c \leq 69$	orthorhombic	*Pbcm*	4

Table 2. Even-Numbered C_{2p}'s Structures as a Function of Chain Length n_c

n_c range	structure	space group	coordination number *Z*
$6 \leq n_c \leq 26$	triclinic	$P\bar{1}$	1
$28 \leq n_c \leq 36$	monoclinic	$P2_1/a$	2
$38 \leq n_c \leq 44$	orthorhombic	*Pbca*	4
$46 \leq n_c \leq 100$	orthorhombic	$Pca2_1$	4

C_n's Structural Behavior versus Temperature. Müller[3] was the first to reveal the existence of solid−solid transitions by X-ray diffraction, when the temperature increases, with the appearance of disordered rotator phases below the melting points of C_n's. From the literature data, Dirand et al.[4] classified these polymorphic transitions according to the behavior described in Schemes 1 and 2 for even- and odd-numbered C_n's, with respect to the increasing temperature.

For the pure C_n's, it is possible to distinguish three categories of polymorphous phases (Schemes 1 and 2): (i) the *ordered phases of low temperatures,* which are the phases stable before the order−order transition toward the ordered phases of high temperatures, (ii) the *ordered phases of high temperatures,* also called crystal phases, observed below the order−disorder transition, and (iii) the *disordered*

* Corresponding author. Telephone: 33.(0)3.83.17.50.07. Fax: 33.(0)3.83.17.50.76. E.mail: mdirand@ensic.inpl-nancy.fr.

10.1021/je0301601 CCC: $25.00
Published on Web 08/30/2003

Scheme 1. Even-numbered C_{2p}'s Phase Succession When the Temperature Increases

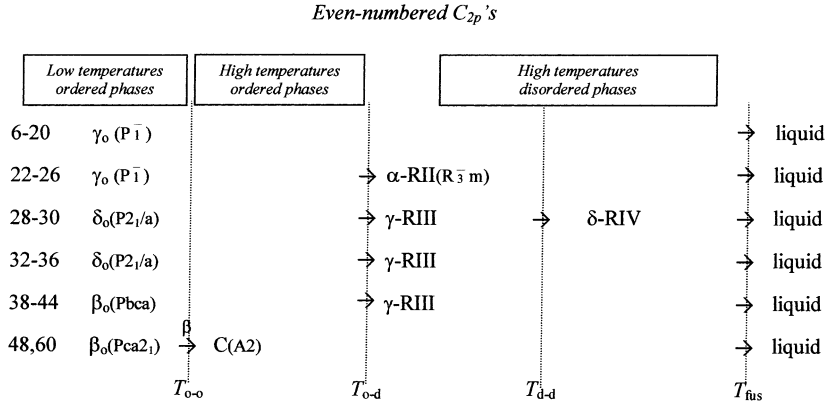

Scheme 2. Odd-Numbered C_{2p+1}'s Phase Succession When the Temperature Increases

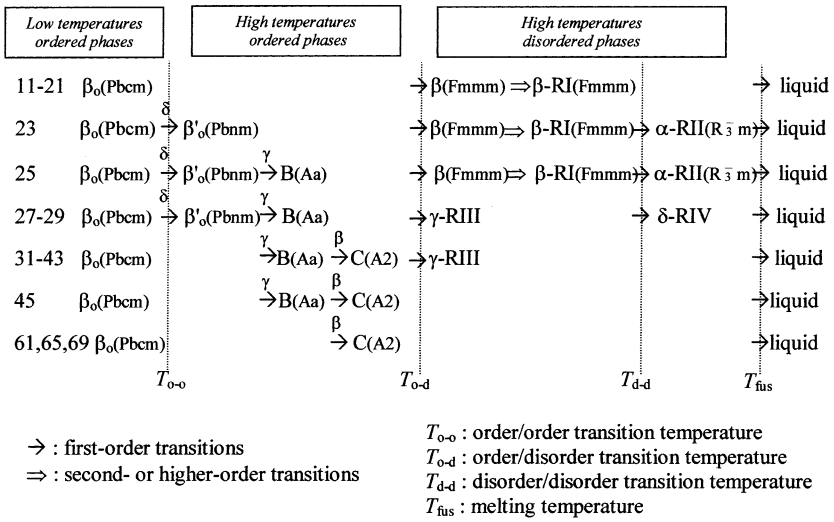

phases of high temperatures, also named rotator or plastic phases. The order−disorder solid−solid transition (hereafter denoted o−d transition) is defined by the higher thermal effect observed at the solid state below the melting point. All these o−d transitions are characterized by important modifications of the molecule orientation around the crystalline *c*-axis (hindered or free rotation), accompanied by the creation of many conformational defects in the molecular chains. We notice that the o−d transition disappears from C_{45}.

Other solid−solid transitions, associated with lower thermal effects, appear, especially for the odd-numbered C_{2p+1}'s:

(i) Order−order transitions below the o−d transition: the transitions δ, β, and γ (cf. C_n structural behavior versus temperature in Scheme 2) lead to high temperature ordered phases whose crystalline structures display differences in the stacking modes of molecule layers along the crystalline *c*-axis and in the concentration of molecule conformational defects per molecule; but any significant modification of the molecule orientation around the *c*-axis is not observed in these ordered phases, contrary to the case for rotator phases.

(ii) Disorder−disorder transitions above the o−d transition: the molecules undergo movements of oscillation around the *c*-axis, whose amplitude progressively increases as a function of the temperature and which generate changes in the stacking sequence of the crystalline planes along the *c*-axis for the β-RI/α-RII transition or in the angle of the molecules' inclination for the γ-RIII/δ-RIV transition.

Temperatures of Solid−Solid Transitions and Fusion

Literature Results. The general review of pure C_n's literature thermodynamic properties has been the topic of a paper by Dirand et al.[4,5] in which all transition temperature data have been collected and averaged from about 60 papers, in a large chain length range going from methane up to C_{390}. The variations of these average temperatures of solid−solid transitions and fusion are reported in Figure 1, as a function of carbon atom number, for the pure C_n's with $8 \leq n_c \leq 45$, and the melting temperature variations are reported in Figure 2 for $4 \leq n_c \leq 390$.

Melting temperature variation as a function of chain length is reported in Figure 2 for C_n's going from methane to C_{390}. The melting temperature variation is asymptotic and tends toward a limit temperature T_0. This asymptotic value T_0 is compared with that of the melting temperature of polyethylene to infinite molecular weight, that is assessed between (407.15 and 411.65) K.[6,7]

Many analytical expressions are available in the literature to represent melting temperature variations with respect to the carbon atom number n_c.[8−15] However, in this study, Broadhurst's model[11] provides the best agreement between literature and calculated melting temperatures (cf.

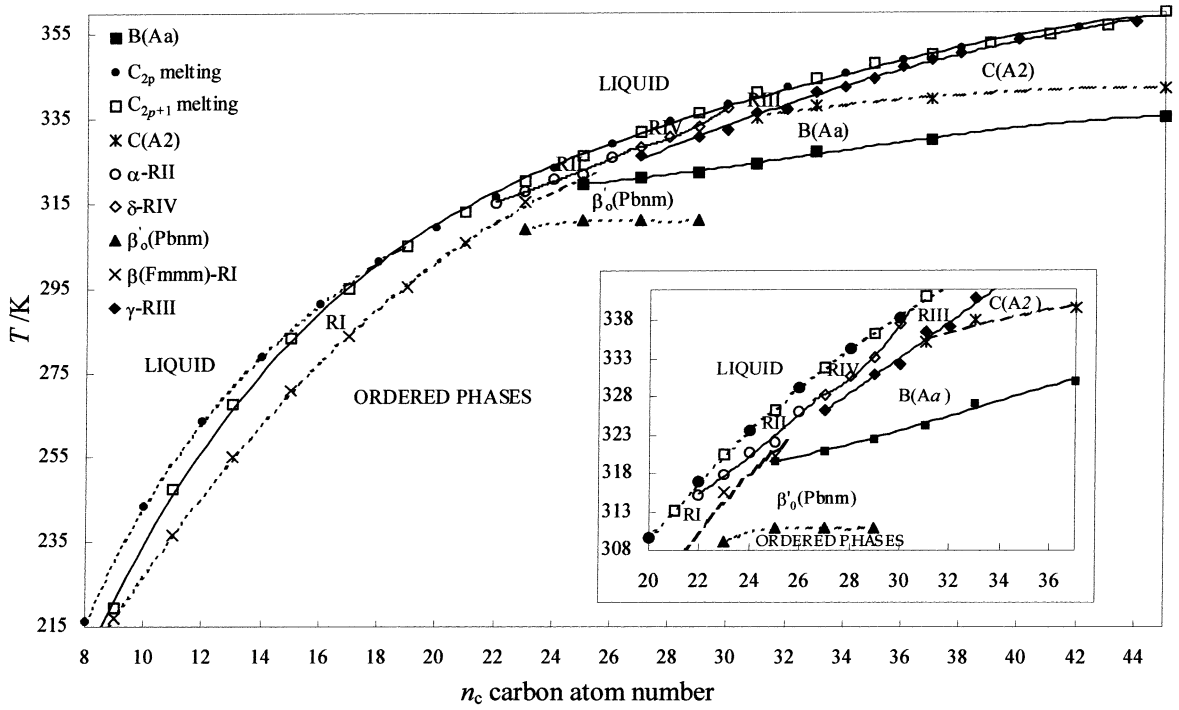

Figure 1. Evolution of solid/solid and solid/liquid transition temperatures[4,5] of pure C_n's versus the carbon atom number n_c ($8 \leq n_c \leq 45$).

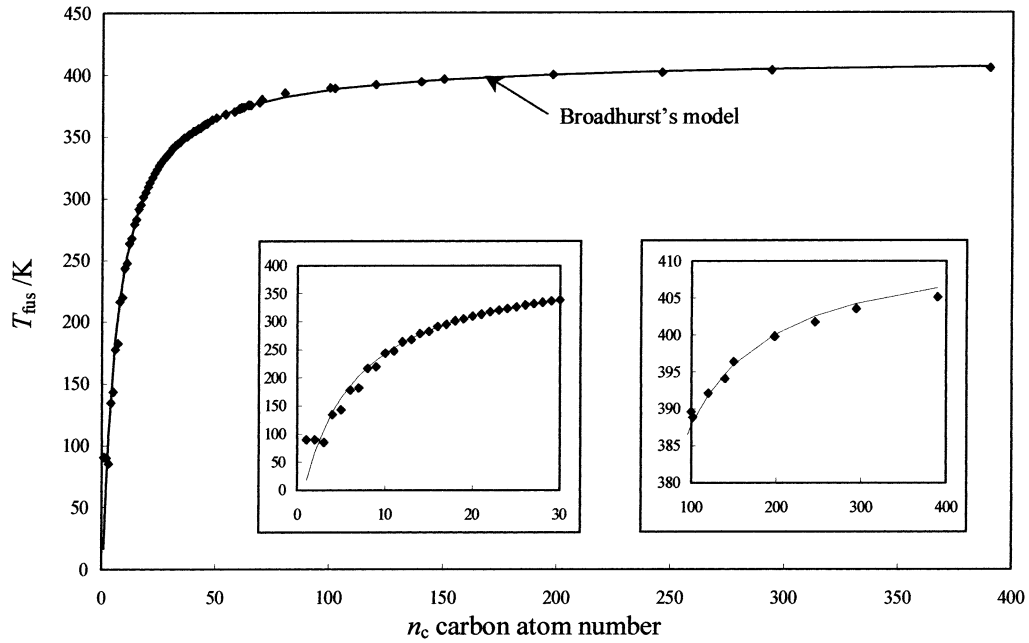

Figure 2. Melting points of pure C_n's: comparison between the mean values of the literature data[4,5] and the calculated values of the Broadhurst model.

Figure 2) for all the C_n's chain length ranges going from methane up to C_{390}. Broadhurst proposed the following expression for the orthorhombic C_n's melting points T_{fus}, as a function of the n_c carbon atom number per molecule:

$$T_{fus}/\mathrm{K} = T_0 \frac{n_c + a}{n_c + b} \qquad (1)$$

with $T_0/\mathrm{K} = \lim_{n_c \to \infty} T_{fus}(n_c)/\mathrm{K}$ the asymptotic value when n_c tends toward infinity.

The fitting of this expression, carried out on the mean data of 67 melting points collected from literature, gives the following values of constants:

$$T_0/\mathrm{K} = \lim_{n_c \to \infty} T_{fus}(n_c)/\mathrm{K} = 413.2, \quad a = -0.725,$$

and $b = 5.754$

New Experimental Results. Although numerous values for temperatures and enthalpies of solid−solid and solid−liquid transitions of pure C_n's are available in the literature, this general review reveals many gaps:

(i) Only some authors[16−19] have carried out measurements of the variations of thermodynamic properties (heat capacities, enthalpies) of light C_n's ($n_c < 27$) versus tem-

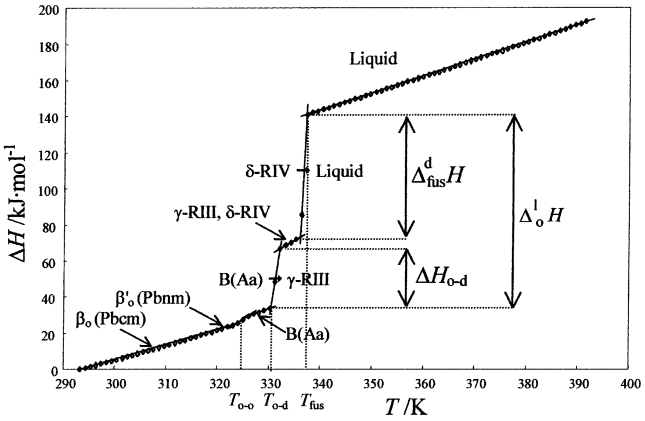

Figure 3. Enthalpy increment curve for the odd-numbered C_{29} from ordered phases of low temperatures up to the liquid phase above the melting point[20] with $\Delta^1_0H = \Delta H_{o-d} + \int_{T_{o-d}}^{T_{fus}} C_{p(R_1)}\,dT + \Delta^d_{fus}H$.

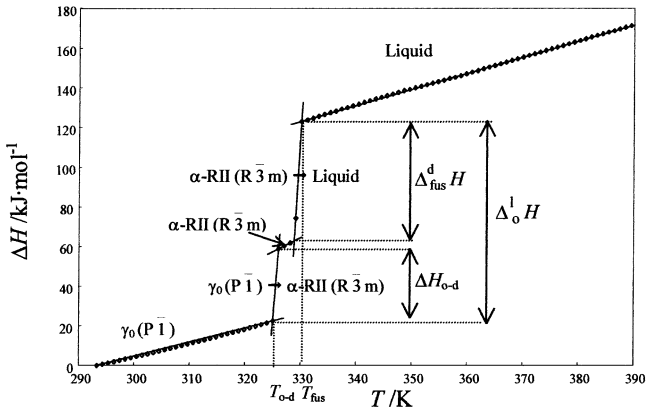

Figure 4. Enthalpy increment curve for the even-numbered C_{26} from ordered phases of low temperatures up to the liquid phase above the melting point[20] with $\Delta^1_oH = \Delta H_{o-d} + \int_{T_{o-d}}^{T_{fus}} C_{p(R_1)}\,dT + \Delta^d_{fus}H$.

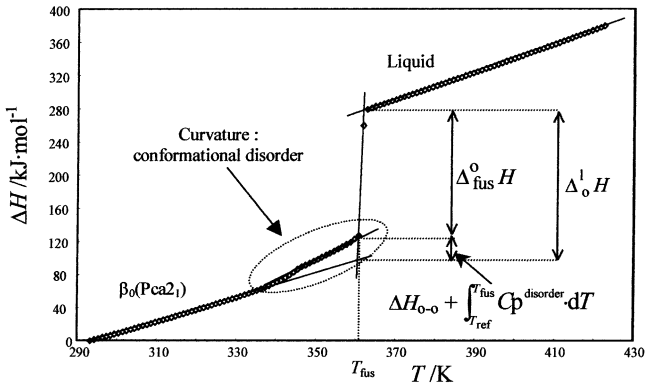

Figure 5. Enthalpy increment curve for the even-numbered C_{46} and for all C_n's with $n_c > 45$ from ordered phases of low temperatures up to the liquid phase above the melting point[20] with $\Delta^1_oH = \Delta H_{o-o} + \int_{T_{ref}}^{T_{fus}} C_p^{disorder}\,dT + \Delta^o_{fus}H$.

perature, from the ordered solid phases of low temperatures up to the liquid phase above the melting point, and these data are even scarcer for the heavy C_n's ($n_c \geq 27$).

(ii) The plurality of the experimental techniques encountered in the literature, combined with thermodynamic data scarcity for heavy C_n's, is responsible for the scattering of some experimental results (especially for heavy C_n's).

So, to remedy to these problems and to have a coherent and reliable set of data, new measurements of the variations of the thermodynamic properties, versus carbon atom number and temperature, have been carried out by differential scanning calorimetry for a large C_n's chain length range including C_n from C_{18} to C_{38} and heavy C_n: C_{41}, C_{44}, C_{46}, C_{50}, C_{54}, C_{60}. These measurements were deduced from differential thermal analyses, performed with a calorimeter of the Tian-Calvet type, using a discontinuous mode of temperature programming with a 1 K temperature jump. The calorimeter device, the operating conditions, and all experimental results (C_n's enthalpy and heat capacity increments from the temperature of ordered phases of low temperatures to the liquid phase above the melting point, temperatures and enthalpies of phase changes) were described in a previous paper,[20] the aim of this study being mainly focused on the establishment of predictive equations, as a function of n_c carbon atom number, by combination of the averaged literature data[4,5] and our own experimental values.[20]

Our experimental variations[20] of transition temperatures with respect to carbon atom number n_c are very similar to those reported in Figures 1 and 2. The fitting of our experimental melting temperature variations by Broadhurst's model gives values for the three parameters T_0, a, and b very close to those previously determined with the literature result set:[4,5]

$$T_0/\mathrm{K} = \lim_{n_c\to\infty} T_{fus}(n_c)/\mathrm{K} = 412.3, \quad a = -0.624, \quad \text{and } b = 5.880 \quad (2)$$

with $T_{fus}/\mathrm{K} = 412.3[(n - 0.624)/(n_c + 5.880)]$.

Enthalpy Variations of Phase Transitions

Generalities. Figures 3−5 show our experimental molar enthalpy increment curves, as a function of the increasing temperature, obtained, respectively, for an odd-numbered C_n (C_{29}) and for a low and a high molecular weight even-numbered C_n (C_{26} and C_{46}) (all the C_n's enthalpy variation tables being provided in a previous paper[20]). In each figure, we have specified, for each transformation, the structural change involved and the temperature limits of transition enthalpy integration. The different transition enthalpies studied involve the following phase changes:

(i) Rotator Phase → Liquid Phase: $\Delta^d_{fus}H$. This enthalpy variation corresponds to the melting of a disordered rotator phase.

(ii) Ordered Phase → Liquid Phase: $\Delta^o_{fus}H$. This transition enthalpy is encountered for the even-numbered C_{2p}'s with $2p \leq 20$ and the odd-numbered C_{2p+1}'s with $2p + 1 \leq 7$ and for all C_n with $n_c \geq 45$, whatever the parity of n_c. For these C_n, which melt without undergoing any solid−solid transition, the ordered phases of low temperatures are stable up to the melting point.

(iii) Ordered Phase → Disordered Phase: ΔH_{o-d}

(iv) Ordered Phase → Liquid Phase: Δ^l_oH (total enthalpy). For this enthalpy variation Δ^l_oH, three carbon atom number ranges must be distinguished: (1) For $n_c(C_{2p+1}) \leq 7$ and $n_c(C_{2p}) < 20$, the lack of polymorphism gives the following equality:

$$\Delta^l_oH = \Delta^o_{fus}H$$

(2) For $9 \leq n_c(C_{2p+1}) < 43$ and $22 < n_c(C_{2p+1}) < 44$, the enthalpy variation between the ordered phase, which is in equilibrium at the o−d transition temperature, and the

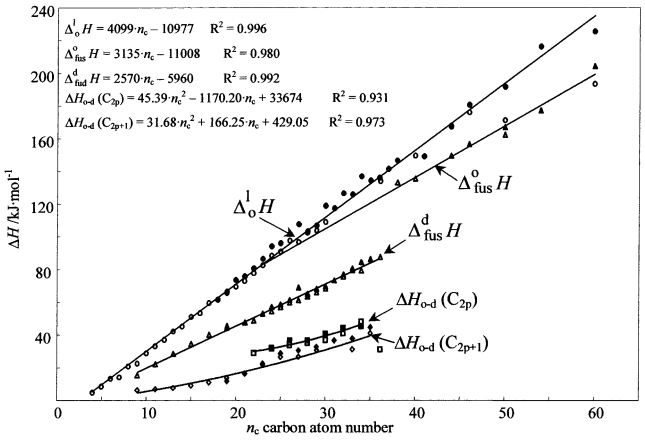

Figure 6. C_n's phase change enthalpies versus carbon atom number n_c: comparison between the mean values of the literature data[4,5] (◇, □, ○) and our experimental values[20] (◆, ■, ●).

liquid phase at the melting point is associated with the sum

$$\Delta_o^l H = \Delta H_{o-d} + \int_{T_{o-d}}^{T_{fus}} C_{p(R_l)}\, dT + \Delta_{fus}^d H + \left(\int_{T_{o-d}}^{T_{d-d}} C_{p(R_1)}\, dT + \Delta H_{d-d} + \int_{T_{d-d}}^{T_{fus}} C_{p(R_2)}\, dT\right) \quad (3)$$

(cf. Figures 3 and 4), with $\int_{T_{o-d}}^{T_{fus}} C_{p(R_l)}\, dT$, $\int_{T_{o-d}}^{T_{d-d}} C_{p(R_l)}\, dT$, and $\int_{T_{d-d}}^{T_{fus}} C_{p(R_2)}\, dT$ being the enthalpy consumptions in the temperature domains of rotator phases and $C_{p(R_1)}$ and $C_{p(R_2)}$, the heat capacities of the disordered rotator phases, differing by their structure.

(3) For $n_c(C_{2p+1}) \geq 45$ and $n_c(C_{2p}) \geq 46$,

$$\Delta_o^l H = \Delta H_{o-o} + \int_{T_{ref}}^{T_{fus}} C_p^{disorder}\, dT + \Delta_{fus}^o H \text{ (cf. Figure 5)} \quad (4)$$

with $\int_{T_{ref}}^{T_{fus}} C_p^{disorder}\, dT$ being the enthalpy consumption induced by the increase of the conformational defect concentration in carbon chains, in the course of heating, and ΔH_{o-o} being the enthalpy variation corresponding to the β order−order transition occurring for heavy C_n, which leads to the appearance of the monoclinic high temperature ordered phase C(A2). The conformational defect development along carbon chains is highlighted by the curvature, depicted in Figure 5, taken by the heat capacity variations in the ordered phases, in the course of heating. This structural defect concentration increases with the temperature and, at a constant temperature value, with the carbon chain length. The enthalpy consumption associated with defect appearance and the order−order transition enthalpy often appear in the same temperature range, and because it is very difficult to separate them successfully, the total enthalpy includes these two enthalpies. Indeed, melting involves an ordered phase which reveals a degree of internal disorder along carbon chains.

Note: The enthalpies of the order−order transition ΔH_{o-o} and the disorder−disorder transition ΔH_{d-d}, which were associated with lower thermal effects, will not be treated in this study.

Phase change enthalpy variations, as a function of carbon atom number, were reported in Figure 6, for the two available sets of data: our experimental measurements,[20] carried out by differential scanning calorimetry for 27 pure C_n's, whose carbon atom numbers are in the C_{18} to C_{60} range, and the literature review mean values,[4,5] in the C_4 to C_{60} range.

We notice a very strong agreement between our experimental enthalpies and the literature transition enthalpies, whatever the carbon atom number, so, we can use these two sets of enthalpy data to optimize the following thermodynamic properties.

Total Enthalpy $\Delta_o^l H$. The values of the $\Delta_o^l H$ enthalpy increase linearly with respect to the n_c carbon atom number, in a manner independent of the n_c parity. The linear equation, as suggested by many authors,[8,12,13,21−23] is established by least-squares fitting of the variations of the total molar enthalpy values

$$\Delta_o^l H/\text{J·mol}^{-1} = 4099 n_c - 10977 \quad (4 \leq n_c \leq 60) \quad (5)$$

The total massic enthalpies were scattered around the following mean value:

$$\Delta_o^l H/\text{J·g}^{-1} = 269 \pm 8 \quad (18 \leq n_c - \leq 60) \quad (6)$$

We notice that our experimental results[20] are slightly higher than those of the literature[4,5] (cf. Figure 6) because of the calorimetric device used: the literature data are obtained by differential thermal analyses, using a continuous mode of temperature programming, and in this last case, it is more difficult to determine with accuracy the baseline of the calorimetric signal in the course of the solid−solid or solid−liquid transitions.

For all C_n's going from C_4 to C_{60}, the total enthalpy $\Delta_o^l H$ values line up, so we can conclude that the disorder mechanisms involved in the o−d transitions are very similar to those occurring during the gradual increasing of heat capacity in the course of heating for heavy C_n's:

(i) For *moderate chain length* C_n's ($9 \leq n_c(C_{2p+1}) \leq 43$ and $22 \leq n_c(C_{2p}) \leq 44$), molecular movement amplification during heating is responsible for the o−d transitions and the occurring of disordered rotator phases, these phases being associated with intermolecular disorder in end methyl group planes perpendicular to carbon chains.

(ii) For *heavy* C_n's ($n_c \geq 45$), which do not undergo any solid−solid transition, the internal disorder grows along carbon chains with a gradual increase of the conformational defect concentration in the course of heating, melting being the answer of the system when the layer stacking becomes unstable.

Note: The ($\Delta H_{o-d} + \Delta_{fus}^d H$) sum often appears in the literature.[19,23−27] However, this sum does not have any physical meaning because the enthalpy variation $\int_{T_{o-d}}^{T_{fus}} C_{p(R)}\, dT$ in the temperature range of disordered phases between T_{o-d} and T_{fus} is not taken into account; nevertheless, that variation is important, especially for the odd-numbered C_{2p+1}'s whose $\beta(Fmmm)$ disordered phase undergoes the rotator-RI second- or higher-order transition with enthalpy consumption and the disorder−disorder transition β-RI($Fmmm$) → α-RII($R\bar{3}m$) (cf. Scheme 2). Thus, the study of $\Delta_o^l H$ enthalpy variations is of major interest and most useful for modeling thermodynamic behavior of C_n's.

Melting Enthalpy $\Delta_{fus}H$. Melting enthalpy variations with respect to carbon atom number n_c (cf. Figure 6) reveal two behaviors according to the chain length range and to the phase change involved in the fusion. Applying the least-squares fitting gives the following linear equations:

(i) for $9 \leq n_c(C_{2p+1}) \leq 35$ and $22 \leq n_c(C_{2p}) \leq 36$:

$$\Delta_{fus}^d H/\text{J·mol}^{-1} = 2570 n_c - 5960 \quad (7)$$

(ii) for $n_c(C_{2p+1}) \geq 45$ and $n_c(C_{2p}) \geq 46$:

$$\Delta^{o}_{fus}H/J\cdot mol^{-1} = 3135n_c - 11008 \quad (8)$$

The melting enthalpy values increase linearly with n_c, whatever the n_c parity. The gap between these two straight lines of $\Delta^{d}_{fus}H$ and $\Delta^{o}_{fus}H$ variations would be equivalent to the o−d transition enthalpy if this latter existed for heavy C_n's ($n_c \geq 45$).

o−d Transition Enthalpy ΔH_{o-d}. The o−d transition enthalpies ΔH_{o-d}, related to the transformation of ordered crystalline phases to disordered rotator phases, show an alternation between even- and odd-numbered C_n's. The explanation of that alternation effect lies in a different polymorphism, as a function of temperature, according to n_c parity. In fact, two carbon atom number ranges must be considered:

(i) *For 22 ≤ n_c < 26:* the odd-numbered C_n's are in the orthorhombic β-RI($Fmmm$) structure while the even-numbered C_n's are in the hexagonal α-RII($R\bar{3}m$) disordered structure just after the o-d transition (cf. Scheme 2). So, this is the sum ($\int_{T_{o-d}}^{T_{d-d}} C_{p(R)}\,dT + \Delta H_{d-d}$), which is not taken into account for C_{2p+1}'s, that generates this alternation.

(ii) *For 27 ≤ n_c ≤ 44:* all C_n's are in the triclinic rotator γ-RIII phase just after the o−d transition, whatever the parity of n_c. The alternation effect is thus induced by the order−order transitions undergone by odd-numbered C_{2p+1}'s, which consume a part of the o−d transition enthalpy by introducing conformational defects.

According to Rajabalee,[28,29] a quadratic expression gives good results for o−d transition enthalpy restitution, after distinction between odd- and even-numbered C_n's:

(i) for $22 \leq n_c(C_{2p}) \leq 36$:

$$\Delta H_{o-d}(C_{2p})/J\cdot mol^{-1} = 45.39{n_c}^2 - 1170.20n_c + 33674.0 \quad (9)$$

(ii) for $9 \leq n_c(C_{2p+1}) \leq 35$:

$$\Delta H_{o-d}(C_{2p+1})/J\cdot mol^{-1} = 31.68{n_c}^2 + 166.25n_c + 429.05 \quad (10)$$

It can be seen that these two curves concur progressively as the carbon atom number increases, with the alternation effect with n_c parity diminishing gradually.

Heat Capacity

Ordered Solid Phase. In ordered solid phases, an expression derived from Einstein's model successfully gives experimental heat capacity variations as a function of temperature.[30−33] In this representation, a C_n molecule behaves like a monatomic solid of N atoms having $3N$ independent vibrations (N being thus the number of oscillators per C_n molecule) which are harmonic and have the same frequency. This frequency corresponds to a typical temperature θ, called Einstein's temperature.

The enthalpy and heat capacity variations can be described by the following expressions:

$$H(T) = \frac{3NR\theta}{\exp(\theta/T) - 1} \quad (11)$$

and

$$C_p(T) \approx C_v(T) = 3NR\left(\frac{\theta}{T}\right)^2 \frac{\exp(\theta/T)}{(\exp(\theta/T) - 1)^2} \quad (12)$$

Nevertheless, these two expressions take into account only the contribution of the group vibrations, and to have a full characterization of C_n's molecular movements, it is also necessary to represent the contribution of the skeletal vibrations (stretching, bending, wagging, twisting, rocking) to thermal energy. By hypothesis, we propose to use, for this skeletal vibration contribution, a quadratic expression that is a function of temperature and carbon chain length. This equation is obtained, from Benson's method of group contribution,[35] by the following steps:

$$C^{C_nH_{2n+2}}_{p(sol)}(T) = 2C^{CH_3}_p(T) + (n_c - 2)C^{CH_2}_p(T)$$

$$C^{C_nH_{2n+2}}_{p(sol)}(T) = 2(A^{CH_3}T + B^{CH_3}T^2) + (n_c - 2)(A^{CH_2}T + B^{CH_2}T^2)$$

$$C^{C_nH_{2n+2}}_{p(sol)}(T) = c(n_c)T + d(n_c)T^2 \quad (13)$$

Thus, the expression of the heat capacity variations becomes

$$C_p(T) = 3NR\left(\frac{\theta}{T}\right)^2 \frac{\exp(\theta/T)}{(\exp(\theta/T) - 1)^2} + cT + dT^2 \quad (14)$$

The parameters N, θ, c, and d are optimized for each C_n by fitting this equation to the experimental enthalpy variations, between 0 K and the first transition temperature, measured by Messerly[16] and Finke[17] for C_n's going from C_5 to C_{18}, by Van Miltenburg[18] for C_{19} and C_{20}, and by Andon[19] for C_{26}. It should be noted that we cannot use our experimental measurements[20] because the lowest temperature reached by our calorimetric device is 283.15 K. The fitted expressions for each parameter, as a function of n_c, are indicated in Table 3. We observe in Figures 7 and 8, showing the molar heat capacity and enthalpy variations versus temperature in the ordered solid phases, a very strong agreement between the values calculated by the expression derived from Einstein's model and the experimental results collected in the literature.[16−19] This agreement is valid in all the chain length ranges studied ($5 \leq n_c \leq 26$) and in almost all the temperature ranges where the solid phase exists. However, the model is no longer applicable for very high temperatures in view of the significant deviation between the experimental and calculated results, and this deviation increases with the increase of the temperature and the C_n's molecular weight. This gap is directly generated by the conformational defect appearance in carbon chains in the course of heating. Indeed, several authors[17,31−34] noticed an abnormal consumption of the C_n's heat capacity in the low temperature ordered solid phases with the approach of the solid−solid transition or melting temperature. This internal disorder development is not taken into account by the model which inevitably underestimates the experimental data for the high temperatures. Since the defect concentration increases with n_c, the model deviation is greater for heavy C_n's (cf. Figures 7 and 8). To sum up, this expression derived from Einstein's model gives very good results for the prediction of C_n's enthalpy and heat capacity variations, in temperature ranges far enough away from the phase transitions.

Liquid Phase. In the liquid phase, all the authors are unanimous in using Benson's method of group contribution for estimating the C_n's thermodynamic properties. Indeed, Benson[35] established a relatively simple, effective, and universal method, which allows us to predict the molar heat capacities of many organic products in the gaseous phase at 298.15 K, by decomposing the molecular structure into

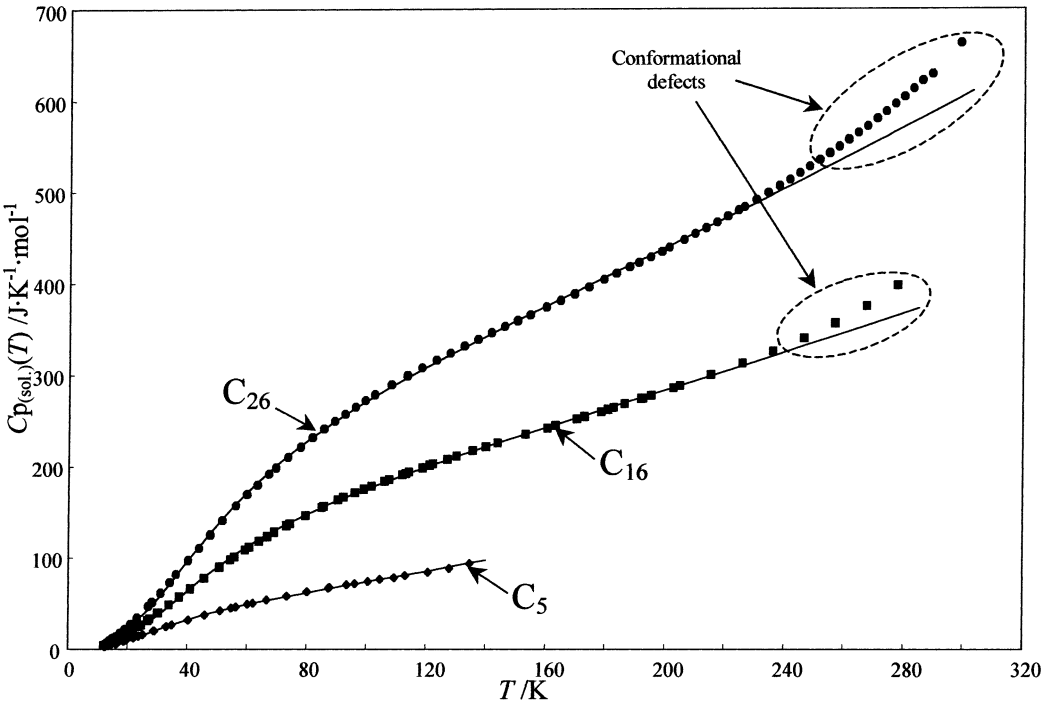

Figure 7. C_n's molar heat capacity variations in the ordered phases, versus temperature and carbon atom number n_c: comparison between the literature data[16−19] (◆, ■, ●) and those calculated by the equation derived from Einstein's model (—).

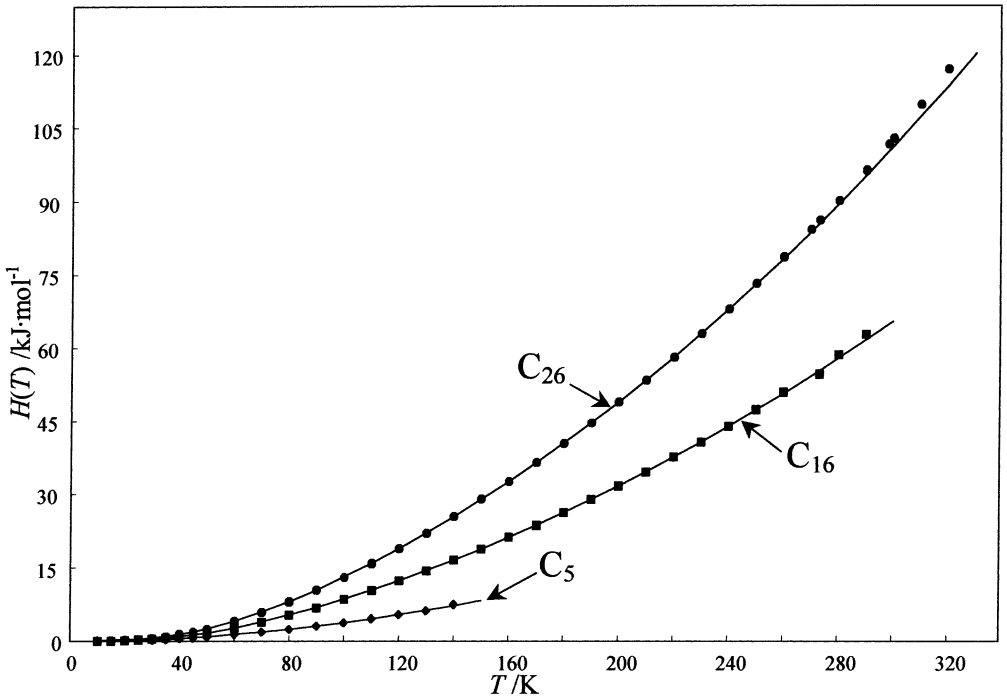

Figure 8. C_n's molar enthalpy variations in the ordered phases, versus temperature and carbon atom number n_c: comparison between the literature data[16−19] (◆, ■, ●) and those calculated by the equation derived from Einstein's model (—).

Table 3. Expressions of Parameters of Eq 14 as a Function of n_c

parameter	expression	R^2	n_c range
$\theta(n_c)$/K	$194.234[(-3.904 \times 10^{-3} + n_c)/(2.772 + n_c)]$	0.997	$5 \le n_c \le 26$
$N\ (n_c)$	$0.306n_c - 0.036$	0.999	$5 \le n_c \le 26$
$c(n_c)$/K^{-2}	$0.034n_c + 0.182$	0.984	$5 \le n_c \le 26$
$d(n_c)$/K^{-3}	$(-5.674 + 36.653/n_c + 0.589n_c) \times 10^{-4}$	0.980	$5 \le n_c \le 26$

characteristic functional groups, whose thermodynamic properties are tabulated. The classification of these different functional groups is made according to their close environment and to the nature of their bonds. By applying this molecular decomposition to the C_n's molecules, the groups to be considered are the (n_c −2) groups CH_2 and the 2 end methyl groups CH_3. The work recently carried out on the heat capacities of pure C_n's in the liquid phase[31,36] suggested that a linear fit can be used, according to the temperature, for the contributions of the groups CH_2

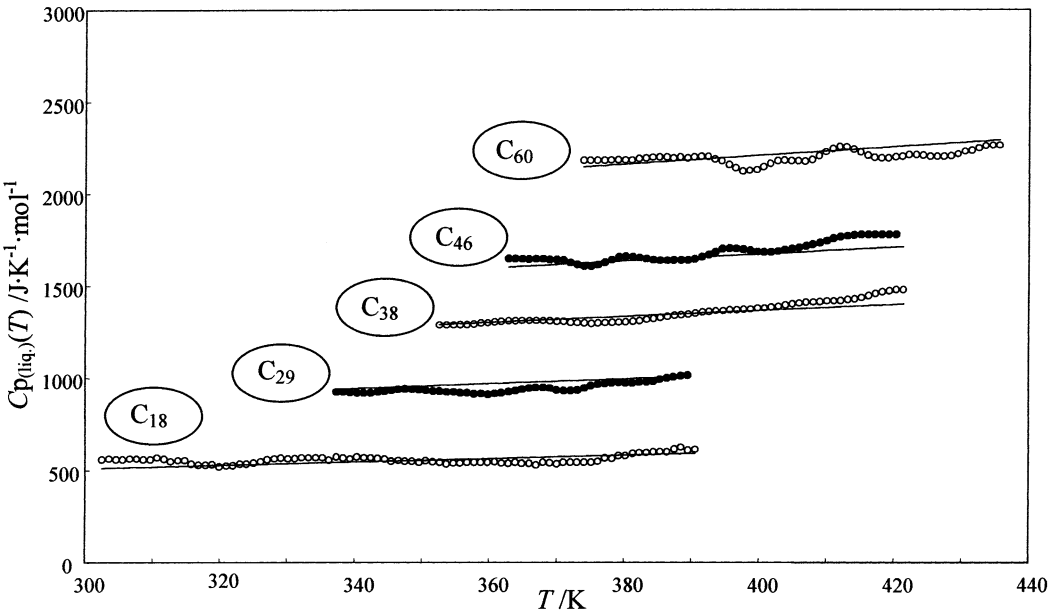

Figure 9. C_n's molar heat capacity variations in the liquid phase, versus temperature and carbon atom number n_c: comparison between the experimental data[20] (○, ●) and those calculated by the model of group contribution (—).

and CH_3. So, the global formula of the C_n's heat capacity in the liquid phase becomes

$$C_{p(liq)}^{C_nH_{2n+2}}(T) = 2(A^{CH_3} + B^{CH_3}T) + (n_c - 2)(A^{CH_2} + B^{CH_2}T) \quad (15)$$

This polynomial relation, as a function of temperature and number of carbon atoms n_c, is obtained by optimization of our experimental measurements[20] of the variations of C_n's heat capacities in the liquid phase, for the 27 pure C_n's studied going from C_{18} to C_{60}:

$$C_{p(liq)}/J\cdot K^{-1}\cdot mol^{-1} = (0.0343n_c + 0.2855)T + 24.587n_c - 203.370 \quad (16)$$

To illustrate the validity of this predictive expression, Figure 9 represents the experimental variations of the heat capacity in the liquid phase of five C_n's[20] and those calculated by Benson's model.

We notice a scattering of the C_n's heat capacity data in the liquid phase, whose amplitude increases with the chain length of the considered C_n (cf. Figure 9). Indeed, this phenomenon of data scattering can be related to a greater internal disorder in high molecular weight C_n's, associated with mechanisms of folding, deformation, and tangling of carbon chains. This explanation was already mentioned by Van Miltenburg[36] and Atkinson,[37] who stated that, in a region of 30−40 K above the melting point, the heat capacities do not follow a linear relationship with temperature. This peculiar behavior would then correspond to the enthalpy necessary to have a completely random orientation of molecules in the liquid phase and break any residual order persisting in the liquid immediately after the melting point.

Conclusion

The combination of a general review of literature data and our calorimetric studies, obtained in a large chain length range, permits the establishment of simple analytical expressions to represent all phase change properties as a function of carbon atom number n_c: linear equations for the total enthalpy and the melting enthalpy and quadratic equations for the o−d transition enthalpy with a distinction between odd- and even-numbered C_n's. In the liquid phase, we proposed a simple function to estimate the heat capacity, by a method of group contribution, for a large range of chain lengths and in strong agreement with the experimental results. For the ordered solid phase, we elaborated a model combining an adaptation of the model of the heat capacity of Einstein's solid, for the vibration aspect of the molecular movements, with a method of group contribution, to take into account the skeletal intramolecular effects. This model effectively restores the heat capacities in a wide domain of temperatures between 0 K and the first temperature of transition. However, it cannot report the peculiar effects related to the increase of the intramolecular defect concentration with the temperature and the C_n's length.

Notation

C_n = *n*-alkane having *n* carbon atoms (C_nH_{2n+2})
n_c = carbon atom number of a C_n molecule
C_{2p} = even-numbered *n*-alkane with *p*, the carbon atom number
C_{2p+1} = odd-numbered *n*-alkane with *p*, the carbon atom number
Z = molecule number by unit-cell (coordination number)

Crystallographic Strucutres

Ordered Phases of n-Alkanes at "Room Temperature"
$\beta_0(C_{2p+1})$ = orthorhombic phase *Pbcm* of odd-numbered C_{2p+1} ($n_c = 2p + 1$)
$\gamma_0(C_{2p})$ = triclinic phase $P\bar{1}$ of even-numbered C_{2p} ($n_c = 2p \leq 26$).
$\delta_0(C_{2p})$ = monoclinic phase $P2_1/a$ of even-numbered C_{2p} ($28 \leq n_c = 2p \leq 36$).
$\beta_0(C_{2p})$ = orthorhombic phase *Pbca* of even-numbered C_{2p} ($38 \leq n_c = 2p \leq 44$).
$\beta_0(C_{2p})$ = orthorhombic phase $Pca2_1$ of even-numbered C_{2p} ($46 \leq n_c = 2p$)

Disordered Phases at "High Temperature"
$\beta(Fmmm)$ = orthorhombic phase; this phase presents the "rotator" state, called β-RI.
α-RII = rhombohedral Rotator phase ($R\bar{3}m$)

γ-RIII = triclinic disorder phase
δ-RIV = monoclinic disorder phase

Thermodynamic Data

a and b = optimization parameters for the relation $T_{fus} = f(n_c)$
T_0 = melting temperature for a C_n with infinite molecular weight
T_{o-o}/K, ΔH_{o-o}/J·mol^{-1} = temperature and enthalpy of the order−order transition
T_{o-d}/K, ΔH_{o-d}/J·mol^{-1} = temperature and enthalpy of the order−disorder transition
T_{fus}/K, $\Delta_{fus}H$/J·mol^{-1} = temperature and enthalpy of the melting
$\Delta_o^1 H$/J·mol^{-1} = total enthalpy variation (ordered phase → liquid)
$\Delta_{fus}^d H$ = melting enthalpy of a disordered rotator phase
$\Delta_{fus}^o H$ = melting enthalpy of an ordered phase
$C_{p(sol)}$, $C_{p(liq)}$/J·K^{-1}·mol^{-1} = heat capacities in the solid and liquid state
$C_{p(R)}$/J·K^{-1}·mol^{-1} = heat capacity in the rotator state
N = number of oscillators per C_n molecule
θ = Einstein's temperature
R = universal gas constant
c/K^{-2}, d/K^{-3} = parameters for the contribution of the skeletal intramolecular effects to energy

Literature Cited

(1) Craig, S. C.; Hastie, G. P.; Roberts, K. J.; Sherwood, J. N. Investigation into the structures of some normal alkanes within the homologous series $C_{13}H_{28}$ to $C_{60}H_{122}$ using high-resolution synchrotron X-ray powder diffraction. *J. Mater. Chem.* **1994**, *4*, 977−981.

(2) Chevallier, V.; Petitjean, D.; Ruffier-Meray, V.; Dirand, M. Correlations between the crystalline long c-parameter and the number of carbon atoms of pure *n*-alkanes. *Polymer* **1999**, *40*, 5953−5956.

(3) Müller, A. An X-ray investigation of normal paraffins near their melting points. *Proc. R. Soc.* **1930**, *A127*, 514−530.

(4) Dirand, M.; Bouroukba, M.; Chevallier, V.; Petitjean, D. Normal alkanes, multialkane synthetic model mixtures, and real petroleum waxes: crystallographic structures, thermodynamic properties and crystallization. *J. Chem. Eng. Data* **2002**, *47*, 115−143.

(5) Dirand, M.; Bouroukba, M.; Briard, A. J.; Chevallier, V.; Petitjean, D.; Corriou, J. P. Temperatures and enthalpies of solid+solid and solid+liquid transitions of *n*-alkanes. *J. Chem. Thermodyn.* **2002**, *34*, 1255−1277.

(6) Chiang, R.; Flory, P. J. Equilibrium between crystalline and amorphous phases in polyethylene. *J. Am. Chem. Soc.* **1961**, *83*, 2857−2862.

(7) Broadhurst, M. G. The melting temperatures of the n-paraffins and the convergence temperature for polyethylene. *J. Res. Natl. Bur. Stand., A: Phys. Chem.* **1966**, *70A*, 481−486.

(8) Garner, W. E.; Van Bibber, K.; King, A. M. CCXI−The melting points and heats of crystallization of the normal long-chain hydrocarbons. *J. Chem. Soc.* **1931**, 1533−1541.

(9) Seyer, W. F.; Patterson, R. F.; Keays, J. L. The density and transition points of the *n*-paraffin hydrocarbons. *J. Am. Chem. Soc.* **1944**, *66*, 179−182.

(10) Broadhurst, M. G. An analysis of the solid-phase behavior of the normal paraffins. *J. Res. Natl. Bur. Stand., A: Phys. Chem.* **1962**, *66A*, 241−249.

(11) Flory, P. J.; Vrij, A. Melting points of linear-chain homologues. The normal paraffin hydrocarbons. *J. Chem. Soc.* **1963**, *85*, 3548−3553.

(12) Dollhopf, W.; Grossmann, H. P.; Leute, U. Some thermodynamic quantities of *n*-alkanes as a function of chain-length. *Colloid Polym. Sci.* **1981**, *259*, 267−278.

(13) Erickson, D. D.; Niesen, V. G.; Brown, T. S.; Conoco Inc. Thermodynamic measurement and prediction of paraffin precipitation in crude oil. *68th Annual Technical Conference and Exhibition of the Society of Petroleum Engineers SPE* **1993**, *26604*, 933−948.

(14) Riazi, M. R.; Daubert, T. E. Characterization parameters for petroleum fractions. *Ind. Eng. Chem. Res.* **1987**, *26*, 755−759.

(15) Riazi, M. R.; Al-Sahhaf, T. A. Physical properties of *n*-alkanes and *n*-alkylhydrocarbons: application to petroleum mixtures. *Ind Eng. Chem. Res.* **1995**, *34*, 4145−4148.

(16) Messerly, J. F.; Guthrie, G. B.; Todd, S. S.; Finke, H. L. Low-temperature thermal data for *n*-pentane, *n*-heptadecane and *n*-octadecane, revised thermodynamic functions for the *n*-alkanes, C_5−C_{18}. *J. Chem. Eng. Data* **1967**, *12*, 338−346.

(17) Finke, H. L.; Gross, M. E.; Waddington, G.; Huffman, H. M. Low-temperature thermal data for the nine normal paraffin hydrocarbons from octane to hexadecane. *J. Am. Chem. Soc.* **1954**, *76*, 333−341.

(18) Van Miltenburg, J. C.; Oonk, H. A.; Metivaud, V. Heat capacities and derived thermodynamic functions of *n*-C_{19} and *n*-C_{20} between 10 K and 390 K. J. *Chem. Eng. Data* **1999**, *44*, 715−720.

(19) Andon, R. J. L.; Martin, J. F. Thermodynamic properties of hexacosane. *J. Chem. Thermodyn.* **1976**, *8*, 1159−1166.

(20) Briard, A. J.; Bouroukba, M.; Petitjean, D.; Hubert, N.; Dirand, M. Experimental enthalpy increments from the solid phases to the liquid phase of homologous *n*-alkane series (C_{18} to C_{38} and C_{41}, C_{44}, C_{46}, C_{50}, C_{60}). *J. Chem. Eng. Data* **2003**, *48*, 497−513.

(21) Barbillon, P.; Schuffenecker, L.; Dellacherie, J.; Balesdent, D.; Dirand, M. Variation d'enthalpie subie de 260 K à 340 K par les n-paraffines, comprises entre l'octadecane (*n*-C_{18}) et l'hexacosane (*n*-C_{26}). *J. Chim. Phys.* **1991**, *88*, 91−113.

(22) Achour, Z.; Sabour, A.; Dirand, M.; Hoch, M. Thermodynamic properties of the *n*-alkanes $C_{19}H_{40}$ to $C_{26}H_{54}$ and their binary phase diagrams. *J. Therm. Anal.* **1998**, *51*, 477−488.

(23) Laux, H.; Butz, T.; Meyer, G.; Matthii, M.; Hildebrand, G. Thermodynamic functions of the solid−liquid transition of hydrocarbons mixtures. *Pet. Sci. Technol.* **1999**, *17*, 897−913.

(24) Schaerer, A. A.; Busso, C. J.; Smith, A. E.; Skinner, L. B. Properties of pure normal alkanes in the C_{17} to C_{36} range. *J. Am. Chem. Soc.* **1955**, *77*, 2017−2019.

(25) Billmeyer, F. W. Lattice energy of crystalline polyethylene. *J. Appl. Phys.* **1957**, *28*, 1114−1118.

(26) Domanska, U.; Wyrzykowska-Stankiewicz, D. Enthalpies of fusion and solid−solid transition of even-numbered paraffins $C_{22}H_{46}$, $C_{24}H_{50}$, $C_{26}H_{54}$ and $C_{28}H_{58}$. *Thermochim. Acta* **1991**, *179*, 265−271.

(27) Srivastava, S. P.; Butz, T.; Oschmann, H. J.; Rahimian, I. Study of the temperature and enthalpy of thermally induced phase-transitions in *n*-alkanes, their mixtures and Fisher-Tropsch waxes. *Pet. Sci. Technol.* **2000**, *18*, 493−518.

(28) Rajabalee, F.; M6tivaud, V.; Mondieg, D.; Haget, Y.; Oonk, H. A. J. Structural and energetic behavior of mixed samples in the hexacosane ($C_{26}H_{54}$)/octacosane (*n*-$C_{28}H_{58}$) system; solid−solid and solid−liquid equilibria. *Helv. Chim. Acta* **1999**, *82*, 1916−1929.

(29) Rajabalee, F.; Metivaud, V.; Oonk, H. A. J.; Mondieg, D.; Waldner, P. Perfect families of mixed crystals: the "ordered" crystalline forms of *n*-alkanes. *Phys. Chem. Chem. Phys.* **2000**, *2*, 1345−1350.

(30) Broadhurst, M. G. Thermodynamic properties of polyethylene predicted from paraffin data. *J. Res. Natl. Bur. Stand., A: Phys. Chem.* **1963**, *67A*, 233−240.

(31) Jin, Y.; Wunderlich, B. Heat capacities of paraffins and polyethylene. *J. Phys. Chem.* **1991,** *95*, 9000−9007.

(32) Achour, Z.; Bouroukba, M.; Balesdent, D.; Provost, E.; Dirand, M. Variation in enthalpy of the system n-tetracosane-n-hexacosane as functions of temperature and composition. *J. Therm. Anal.* **1997,** *50*, 685−704.

(33) Jouti, B.; Bouroukba, M.; Balesdent, D.; Dirand, M. Enthalpy variation of the nine solids phases of the binary molecular alloys (n-tricosane: *n*-pentacosane) vs temperature. *J. Therm. Anal.* **1998**, *54*, 785−802.

(34) Ubbelohde, A. R. Structure and thermodynamic properties of long-chain compounds. *Trans. Faraday Soc.* **1938,** *34*, 282−299.

(35) Benson, S. W.; Cruickshank, F. R.; Golden, D. M.; Haugen, G. R.; O'Neal, H. E.; Rodgers, A. S.; Shaw, R.; Walsh, R. Additivity rules for the estimation of thermochemical properties. *Chem. Rev.* **1969,** *69*, 279−295.

(36) Van Miltenburg, J. C. Fitting the heat capacity of liquid *n*-alkanes: new measurements of *n*-heptadecane and *n*-octadecane. *Thermochim. Acta* **2000**, *343*, 57−62.

(37) Atkinson, C. M. L.; Larkin, J. A.; Richardson, M. J. Enthalpy changes in molten *n*-alkanes and polyethylene. *J. Chem. Thermodyn.* **1969**, *1*, 435−440.

Received for review March 26, 2003. Accepted July 18, 2003.

JE0301601